References

1. Dunnill MS. The pathology of asthma, with special reference to changes in the bronchial mucosa. *J Clin Pathol* 1960;13:27–33.
2. Vrugt B, Wilson S, Bron A, Holgate ST, Djukanovic R, Aalbers R. Bronchial angiogenesis in severe glucocorticoid-dependent asthma. *Eur Respir J* 2000;15:1014–1021.
3. Hashimoto M, Tanaka H, Abe S. Quantitative analysis of bronchial wall vascularity in the medium and small airways of patients with asthma and COPD. *Chest* 2005;127:965–972.
4. Mostaço-Guidolin LB, Osei ET, Ullah J, Hajimohammadi S, Fouadi M, Li X, *et al*. Defective fibrillar collagen organization by fibroblasts contributes to airway remodeling in asthma. *Am J Respir Crit Care Med* 2019;200:431–443.
5. Mostaco-Guidolin L, Hajimohammadi S, Vasilescu DM, Hackett T.-L. Application of Euclidean distance mapping for assessment of basement membrane thickness distribution in asthma. *J Appl Physiol (1985)* 2017; 123:473–481.
6. Schindelin J, Arganda-Carreras I, Frise E, Kaynig V, Longair M, Pietzsch T, *et al*. Fiji: an open-source platform for biological-image analysis. *Nat Methods* 2012;9:676–682.
7. Rydell-Törmänen K, Johnson JR, Fattouh R, Jordana M, Erjefält JS. Induction of vascular remodeling in the lung by chronic house dust mite exposure. *Am J Respir Cell Mol Biol* 2008;39:61–67.
8. Saetta M, Di Stefano A, Rosina C, Thiene G, Fabbri LM. Quantitative structural analysis of peripheral airways and arteries in sudden fatal asthma. *Am Rev Respir Dis* 1991;143:138–143.
9. Avdalovic M. Pulmonary vasculature and critical asthma syndromes: a comprehensive review. *Clin Rev Allergy Immunol* 2015;48:97–103.
10. Asosingh K, Swaidani S, Aronica M, Erzurum SC. Th1- and Th2-dependent endothelial progenitor cell recruitment and angiogenic switch in asthma. *J Immunol* 2007;178:6482–6494.
11. Santos S, Peinado VI, Ramírez J, Melgosa T, Roca J, Rodriguez-Roisin R, *et al*. Characterization of pulmonary vascular remodelling in smokers and patients with mild COPD. *Eur Respir J* 2002;19:632–638.
12. Daley E, Emson C, Guignabert C, de Waal Malefyt R, Louten J, Kurup VP, *et al*. Pulmonary arterial remodeling induced by a Th2 immune response. *J Exp Med* 2008;205:361–372.
13. Ash SY, Rahaghi FN, Come CE, Ross JC, Colon AG, Cardet-Guisasola JC, *et al*.; SARP Investigators. Pruning of the pulmonary vasculature in asthma: the severe asthma research program (sarp) cohort. *Am J Respir Crit Care Med* 2018;198:39–50.

Efficient Transduction of Alveolar Type 2 Cells with Adeno-associated Virus for the Study of Lung Regeneration

To the Editor:

Gene transfer to alveolar type 2 (AT2) cells provides unique opportunities to study and correct monogenetic interstitial lung diseases (ILDs); however, efficient and cell-selective gene transfer to AT2 cells has proven challenging. The most effective and commonly used gene delivery vectors are those based on adeno-associated virus (AAV). AAVs are small, nonenveloped, single-stranded DNA parvoviruses capable of transducing nondividing cells (1, 2), making them ideal candidates to target the alveolar epithelium, wherein <0.5% of alveolar cells are actively dividing (3). AAV capsid binding to cell surface receptors on target cells mediates the cell selectivity of AAV serotypes 1–9. AAV6 binds N-linked sialic acid (1, 2). Sialic acid sugars are abundant on the apical surface of airway cells, consistent with AAV6 being highly effective in transducing airway epithelial cells (1, 2, 4, 5).

Phosphorylation of tyrosine residues in endocytosed AAV capsids by epidermal growth factor receptor protein tyrosine kinase is a prerequisite for ubiquitination, which marks capsids for degradation by cytoplasmic proteasomes (6). However, mutation of exposed capsid tyrosine residues blocks ubiquitin-mediated degradation, leading to enhanced transgene expression (6, 7). To increase lung specificity and enhance transgene expression, we engineered mutation of tyrosine residues 445 and 731 to phenylalanine (Y445F and Y731F) in the AAV6.2 capsid, termed "AAV6.2FF" (F129L, Y445F, and Y731F). Our recent data indicate that AAV6.2FF capsid enhanced transgene expression nearly 10-fold compared with AAV6 and enabled correction of lethal surfactant protein B deficiency *in vivo* (8, 9).

To identify the cell-type specificity of AAV6.2FF, we produced an AAV6.2FF-expressing mCherry (AAV6.2FF-mCherry). After intranasal administration, AAV6.2FF-mCherry transduced ~50–90% of $CD326^+$ epithelial cells over a wide range of doses 2 weeks after infection, whereas it only transduced ~20% of $CD45^+$ immune cells (Figures 1A, E1A, and E1B). By immunofluorescence, ~80% of $mCherry^+$ cells were $proSPC^+NKX2.1^+HOPX^-$ AT2 cells (Figure 1B, E1C, and E1D). Less than 0.5% of $mCherry^+$ cells were $HOPX^-$ alveolar type 1 cells (Figures E1 C and E1D), and <5% of $mCherry^+$ cells were $CD45^+$ immune cells (Figures E1C and E1D). The $mCherry^+$ cells were not identified by antibody staining in proximal airway ciliated, club, and goblet cells; however, $mCherry^+$ cells were identified in terminal bronchioles and alveoli 2 weeks after transduction (Figure E2). Conversely, $LacZ^+$ epithelial cells in proximal epithelial cells of Rosa-LacZ mice were observed after AAV6.2FF-Cre administration (8), suggesting that AAV6.2FF-driven transgenes are expressed at lower concentrations in proximal epithelial cells compared with AT2 cells and therefore require enzyme/substrate-based signal amplification systems for detection.

To test whether the efficiency of AT2 cell targeting was influenced by the transgene cassette, we developed AAV6.2FF-GFP, which transduced 75% of $CD326^+$ epithelial cells (Figure E3). AAV6.2FF targeting of alveolar AT2 cells did not alter lung histopathology or cause alveolar inflammation (Figure E4). Taken together, these data demonstrate that AAV6.2FF efficiently and selectively transduced ~80% of alveolar AT2 cells in peripheral mouse lung without causing lung injury 2 weeks after transduction.

The study of monogenetic disorders affecting AT2 cell function and causing ILD is limited by the time and expense needed to produce transgenic mice bearing AT2 cell–specific promoter constructs to delete or mutate genes of interest. To eliminate the need for biallelic transgenic mice, we produced an AAV6.2FF-Cre to express Cre-recombinase in AT2 cells. To test the efficacy of AAV6.2FF-Cre in mouse lung AT2 cells, floxed-tdTomato reporter mice [$Gt(ROSA)26Sor^{tm14(CAG-tdTomato)Hze}$; 007909; Jackson Labs] were treated with AAV6.2FF-Cre. Two weeks after transduction with AAV6.2FF-Cre, Cre-mediated activation of tdTomato was identified in 60–80% of $CD326^+$ epithelial cells (Figures 1C and E5A), consistent with our previous data using a LacZ reporter (8). AAV6.2FF-Cre–mediated activation of tdTomato in AT2 cells did not cause adverse lung histopathology (Figure E5B). After AAV6.2FF-Cre transduction, $tdTomato^+$ cells were quantitated by

Supported by National Institutes of Health HL131634 (J.P.B.) and HL13475 (J.A.W.)

This letter has a data supplement, which is accessible from this issue's table of contents at www.atsjournals.org.

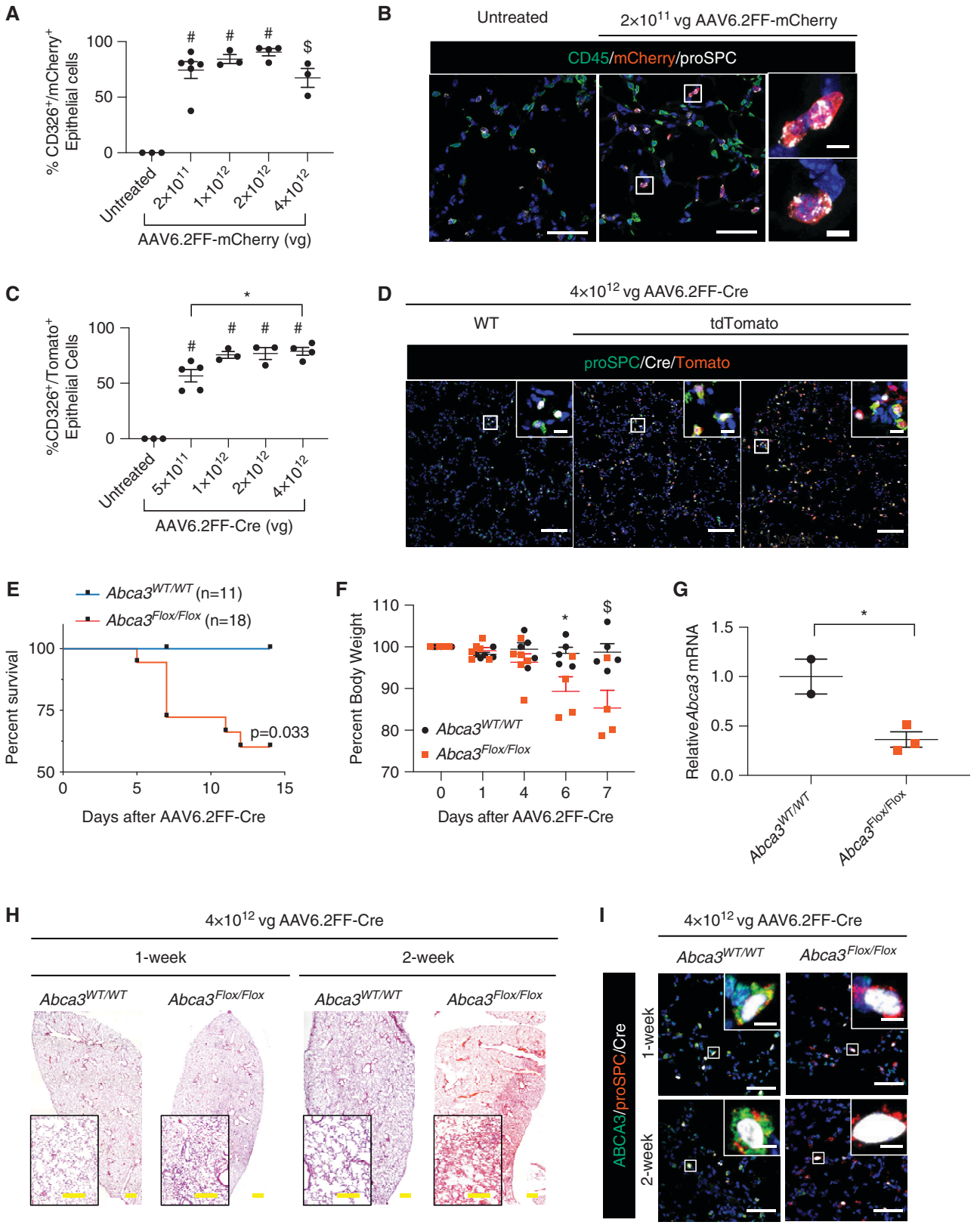

Figure 1. AAV6.2FF transduction of pulmonary epithelial cells. (*A* and *B*) C57Bl/6 mice were administered 2×10^{11} – 4×10^{12} viral genomes (vg) of AAV6.2FF-mCherry intranasally, and mCherry expression was analyzed in whole lungs 2 weeks later by flow cytometry identifying $CD326^+$ epithelial cells (*A*) and confocal immunofluorescence staining (*B*) for CD45 (green), mCherry (red), and proSPC (white). Data are expressed as

immunofluorescence staining; ~80% of proSPC$^+$ AT2 cells were tdTomato$^+$ (Figures 1D and E5C). Taken together, these findings indicate that AAV6.2FF-Cre is highly effective in causing Cre-mediated recombination of reporter genes in AT2 cells *in vivo*.

Mutation of human *ABCA3* or deletion of *Abca3* in mice causes alveolar injury and remodeling, leading to respiratory failure and death (3). To determine whether AAV6.2FF-Cre could efficiently delete a disease-linked gene in AT2 cells, we transduced *Abca3*$^{Flox/Flox}$ mice with AAV6.2FF-Cre. *Abca3*$^{Flox/Flox}$ mice administered AAV6.2FF-Cre intranasally developed signs of respiratory failure, including dehydration, dyspnea, and hunched appearance, accompanied by significant weight loss 7 days after transduction, requiring euthanasia or causing death within 5–14 days (Figure 1E-F). These pathophysiological effects were comparable with those observed using a genetic deletion approach with a *Sftpc*CreER allele (3). ABCA3 staining of Cre$^+$ AT2 cells (proSPC$^+$) after AAV6.2FF-Cre administration was markedly decreased in *Abca3*$^{Flox/Flox}$ mice (Figure 1I), consistent with a 70% loss of *Abca3* mRNA in whole lung 1 week after transduction (Figure 1G). The loss of ABCA3 was accompanied by pulmonary inflammation and septal wall thickening 1 and 2 weeks after transduction (Figure 1H). After extensive loss of *Abca3,* mice developed respiratory failure and death, consistent with the requirement of ABCA3 for lung function in newborn infants (3). These findings demonstrate the efficacy of AAV6.2FF-Cre to model monogenetic disorders of surfactant deficiency, bypassing the need for conditional AT2-specific Cre transgenic mouse lines. Some inducible Cre transgenic mouse lines produce tamoxifen-independent recombination events that are not tightly controlled (3); however, AAV6.2FF-Cre permits tightly controlled temporal expression of Cre-recombinase in AT2 cells *in vivo*.

To determine whether the AAV6.2FF system could be used to inhibit gene expression in AT2 cells, we generated a cassette containing three unique microRNAs (miRs) in tandem that target *Sftpc* mRNA. Western blot analysis of whole lung 7 days after transduction showed a >90% reduction of pro-SFTPC protein, demonstrating the efficacy of the miR-based system to target gene expression in AT2 cells *in vivo* (Figure E6).

In summary, we identified cell-type selectivity of the AAV6.2FF capsid in mouse lung, demonstrating transgene expression in epithelial cells of terminal bronchioles and alveoli, with lower expression in larger airways 2 weeks after transduction. In peripheral lung, AAV6.2FF-driven transgenes were expressed in ~80% of CD326$^+$ epithelial cells without alveolar inflammation or adverse lung histopathology. At present, the mechanisms underlying higher transgene expression in peripheral versus proximal epithelial cells is unknown. AAV6.2FF is a useful tool for gene transfer and inhibition for the study of lung formation and disease pathogenesis.

Author disclosures are available with the text of this letter at www.atsjournals.org.

Tara N. Rindler, Ph.D.
Kari M. Brown, B.A.
Cincinnati Children's Hospital Medical Center
Cincinnati, Ohio

Courtney A. Stockman, B.S.
Stanford University
Stanford, California

Laura P. van Lieshout, Ph.D.
University of Guelph
Guelph, Ontario, Canada

Emily P. Martin, B.S., M.S.
Timothy E. Weaver, M.S., Ph.D.
William J. Zacharias, M.D., Ph.D.
Cincinnati Children's Hospital Medical Center
Cincinnati, Ohio

Sarah K. Wootton, M.Sc., Ph.D.
University of Guelph
Guelph, Ontario, Canada

Jeffrey A. Whitsett, M.D.
Cincinnati Children's Hospital Medical Center
Cincinnati, Ohio

James P. Bridges, Ph.D.*
National Jewish Health
Denver, Colorado

ORCID IDs: 0000-0003-0384-6434 (T.N.R.); 0000-0003-1668-5174 (J.A.W.); 0000-0002-4815-117X (J.P.B.).
*Corresponding author (e-mail: bridgesj@njhealth.org)

Figure 1. *Continued.* mean ± SE; $n = 3$–6 mice/group. $^{\$}P < 0.001$ and $^{\#}P < 0.0001$ as determined by one-way ANOVA. (*C* and *D*) Gt(ROSA)26Sor$^{tm14(CAG-tdTomato)Hze}$ (tdTomato) mice were administered 5×10^{11} – 4×10^{12} vg AAV6.2FF-Cre intranasally, and expression of tdTomato was analyzed in whole lungs 2 weeks later by flow cytometry identifying CD326$^+$ epithelial cells (*C*) and confocal immunofluorescence staining (*D*) for proSPC (green), tdTomato (red), and Cre (white). Data are expressed as mean ± SE; $n = 3$–5 mice/group. $^{*}P < 0.05$ and $^{\#}P < 0.0001$ as determined by one-way ANOVA. (*E*–*I*) *Abca3*$^{WT/WT}$ or *Abca3*$^{Flox/Flox}$ mice were administered 4×10^{12} vg of AAV6.2FF-Cre intranasally, and lungs were analyzed histologically 1 and 2 weeks later. (*E*) Kaplan-Meier curve for survival and statistical analysis (Wilcoxon-Gehan test). (*F*) Percentage body weight after AAV6.2FF-Cre administration. Data are expressed as mean ± SE; $n = 4$–5 mice/group. $^{*}P < 0.05$ and $^{\$}P < 0.001$ as determined by one-way ANOVA. (*G*) Quantitative PCR of *Abca3* mRNA in whole lung at 1 week after transduction. Data are expressed as mean ± SE; $n = 2$–6 mice/group. $^{*}P < 0.05$ as determined by unpaired Student's *t* test. (*H*) Representative lung histology is shown. (*I*) Representative confocal immunofluorescence staining for ABCA3 (green), proSPC (red), and Cre (white). Scale bars: *A* and *I*, 50 μm; insert scale bars, 5 μm; *D*, 100 μm; insert scale bars, 10 μm; *H*, 500 μm; insert scale bar, 250 μm.

References

1. Zincarelli C, Soltys S, Rengo G, Rabinowitz JE. Analysis of AAV serotypes 1-9 mediated gene expression and tropism in mice after systemic injection. *Mol Ther* 2008;16:1073–1080.
2. Ellis BL, Hirsch ML, Barker JC, Connelly JP, Steininger RJ III, Porteus MH. A survey of ex vivo/in vitro transduction efficiency of mammalian primary cells and cell lines with Nine natural adeno-associated virus (AAV1-9) and one engineered adeno-associated virus serotype. *Virol J* 2013;10:74.
3. Rindler TN, Stockman CA, Filuta AL, Brown KM, Snowball JM, Zhou W, *et al.* Alveolar injury and regeneration following deletion of ABCA3. *JCI Insight* 2017;2:e97381.
4. Limberis MP, Vandenberghe LH, Zhang L, Pickles RJ, Wilson JM. Transduction efficiencies of novel AAV vectors in mouse airway epithelium in vivo and human ciliated airway epithelium in vitro. *Mol Ther* 2009;17:294–301.
5. Seiler MP, Miller AD, Zabner J, Halbert CL. Adeno-associated virus types 5 and 6 use distinct receptors for cell entry. *Hum Gene Ther* 2006;17:10–19.
6. Zhong L, Li B, Jayandharan G, Mah CS, Govindasamy L, Agbandje-McKenna M, *et al.* Tyrosine-phosphorylation of AAV2 vectors and its consequences on viral intracellular trafficking and transgene expression. *Virology* 2008;381:194–202.
7. Yan Z, Zak R, Luxton GW, Ritchie TC, Bantel-Schaal U, Engelhardt JF. Ubiquitination of both adeno-associated virus type 2 and 5 capsid proteins affects the transduction efficiency of recombinant vectors. *J Virol* 2002;76:2043–2053.
8. Kang MH, van Lieshout LP, Xu L, Domm JM, Vadivel A, Renesme L, *et al.* A lung tropic AAV vector improves survival in a mouse model of surfactant B deficiency. *Nat Commun* 2020;11:3929.
9. van Lieshout LP, Domm JM, Rindler TN, Frost KL, Sorensen DL, Medina SJ, *et al.* A Novel Triple-Mutant AAV6 Capsid Induces Rapid and Potent Transgene Expression in the Muscle and Respiratory Tract of Mice. *Mol Ther Methods Clin Dev* 2018;9:323–329.

Erratum: Lung Expression of Human Angiotensin-Converting Enzyme 2 Sensitizes the Mouse to SARS-CoV-2 Infection

There is an error in the article by Han and colleagues (1), published in the January 2021 issue of the *Journal*. The authors inadvertently omitted the following text, which should have appeared in an ACKNOWLEDGMENT section:

The authors thank Ms. Kejing Song, who performed the bulk-RNAseq library preparation and next-generation sequencing for this article at the Tulane Center for Translational Research in Infection and Inflammation on the Illumina NGS core (https://medicine.tulane.edu/centers-institutes/tulane-ctrii/nextgen-sequencing).

Reference

1. Han K, Blair RV, Iwanaga N, Liu F, Russell-Lodrigue KE, Qin Z, Midkoff CC, Golden NA, Doyle-Meyers LA, Kabir ME, Chandler KE, Cutrera KL, Ren M, Monjure CI, Lehmicke G, Fischer T, Beddingfield B, Wanek AG, Birnbaum A, Maness NJ, Roy CJ, Datta PK, Rappaport J, Kolls JK, Qin X. Lung expression of human angiotensin-converting enzyme 2 sensitizes the mouse to SARS-CoV-2 infection. *Am J Respir Cell Mol Biol* 2021;64:79–88.